Spectrochimica Acta Part A 93 (2012) 348–353

Contents lists available at SciVerse ScienceDirect

Spectrochimica Acta Part A: Molecular and Biomolecular Spectroscopy

journal homepage: www.elsevier.com/locate/saa

Spectral and *in vitro* antimicrobial properties of 2-oxo-4-phenyl-6-styryl-1,2,3,4-tetrahydro-pyrimidine-5-carboxylic acid transition metal complexes

Raksha P. Dhankar[a], Anjali M. Rahatgaonkar[b,*], Mukund S. Chorghade[c], Ashutosh Tiwari[d,*]

[a] *Department of Chemistry, Sardar Patel Mahavidyalaya, Ganjward, Chandrapur 442402, Maharashtra, India*
[b] *Chemistry Department, Institute of Science, Civil Lines, Nagpur 440001, Maharashtra, India*
[c] *Chorghade Enterprises, 14 Carlson Circle, Natick, MA, USA*
[d] *Biosensors and Bioelectronics Centre, Institute of Physics, Chemistry and Biology, Linköping University, S-58183 Linköping, Sweden*

ARTICLE INFO

Article history:
Received 6 August 2011
Received in revised form 21 February 2012
Accepted 23 February 2012

Keywords:
Pyrimidine transition metal complexes
Spectral
Octahedral
Square planar geometry
Anti-microbial activity

ABSTRACT

2-oxo-4-phenyl-6-styryl-1,2,3,4-tetrahydro-pyrimidine-5-carboxylic acid (ADP) was complexed with acetates of Mn(II), Ni(II), Cu(II) and Zn(II). The structures of the ligand and its metal complexes were characterized by microanalysis, IR, NMR, UV–vis spectroscopy, magnetic susceptibility and TGA–DTA analyses. Octahedral and square planar geometries were suggested for the complexes in which the central metal ion coordinated with —O donors of ligand and acetate ions. Each ligand binds the metal using carboxylate oxygens. The ligand and complexes were evaluated for their antimicrobial activities against different species of pathogenic bacteria and fungi. The present novel pyrimidine containing complexes could constitute a new group of antibacterial and antifungal agents.

1. Introduction

The design of ligands is an important part of the synthetic repertoire of chemists. It gets *via* subtle control coordination of ligands on a metal centre [1–3]. Ligands contain significantly different chemical functionalities, such as hard and soft donors, often called hybrid ligands that find utility in molecular chemistry [4–6]. The incorporation of pyrimidine moieties in multifunctional ligands of increasing complexity makes for excellent complexation; have rarely been documented in pyrimidine chemistry [7]. The coordination chemistry of pyrimidine derived ligands is of relevance due to their biological implications.

In general, the three dimensional coordination of metal with ligands allows molecule to identify and interact with definite site of the target bio-molecules. Also, deviation in the oxidation state of transition metal is important feature for the bio-redox chemistry. The exchange processes of metal complexes permit the bio-molecule to interact and coordinate with metals centre [8]. The systematic study of metal based bio-active complex are summarized with (i) the active entire inert complex, (ii) the active entire reactive complex, (iii) a active fragment of the complex, (iv) the active metal ion or one of its bio-transformation products, (v) the enhancer metal after radiation, (vi) the radioactive metal, and (vii) responsible for the bio-activity *via* one or more of the ligands [9].

In recent years, a number of studies have reported on synthesis and structural analysis of metal complexes of pyrimidine containing bi- and tri-dentate ligands (ONO donors) having microbial activity, *i.e.*, from donor ligands and complexes [10,11]. Pyrimidines are endowed with a wide range of biological activities [12–15]. The chelation of metal ions with pyrimidine ring enhances their activities due to easy availability of potential sites for binding. The complexed metal ions give information on their coordination properties and insights towards understanding the role of metal ions in the biological systems [17]. Herein, we expand on the scope of pyrimidine ligands, emphasize hybrid ligands, and explain the synergies obtained by combining these two facets of ligand design. The synthesis and physical properties of new Ni(II), Cu(II) and Zn(II) pyrimidine complexes were determined and the ligands investigated for potential microbial activities.

2. Experimental

2.1. Materials

Benzaldehyde (Qualigen Fine Chemicals, 99.9%), ethylacetoacetate (Qualigen Fine Chemicals, 99%), urea (Qualigen Fine

* Corresponding authors.
E-mail addresses: anjali_rahatgaonkar@yahoo.com (A.M. Rahatgaonkar), ashutosh.tiwari@liu.se, ashtiwa@gmail.com (A. Tiwari).

1386-1425/$ – see front matter © 2012 Elsevier B.V. All rights reserved.
doi:10.1016/j.saa.2012.02.096

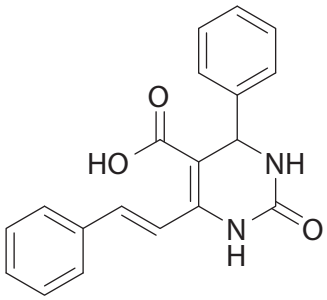

Fig. 1. Chemical structure of 2-oxo-4-phenyl-6-styryl-1,2,3,4-tetrahydro-pyrimidine-5-carboxylic acid (ADP).

Chemicals, 99.8%), sodium hydroxide (Qualigen Fine Chemicals, 99%) and metal acetates (Qualigen Fine Chemicals, 99.9%) were used without further purification. All supplementary chemicals were of analytical grade and aqueous solutions were prepared with sterilized Milli-Q water (18.2 Ω/cm^2).

2.2. Synthesis of ligand (E)-2-oxo-4-phenyl-6-styryl-1,2,3,4-tetrahydro-pyrimidine-5-caboxylic acid (ADP)

A mixture of 6-methyl-2-oxo-4-phenyl-1,2,3,4-tetrahydro-pyrimidine-5-carboxylic ethyl ester (1.9 mM, 500 mg), and 25 mL of 10% NaOH was refluxed for 4 h [18]. It was cooled and poured into 20% HCl solution, filtered and washed with water. The solid obtained was recrystallized from ethanol. Yield, 70%; m.p. 220 °C [19,20]. Anal. Calcd for $C_{19}H_{16}N_2O_3$: C, 71.23; H, 5.0; N, 8.74. Found (%): C, 71.56; H; 5.10, N, 8.76. IR data: (KBr, λ_{max}/cm^{-1}) 3410 (N—H), 3231 (N—H), 3115 (O—H), 1685 (C=O), 970 (CH=CH) cm^{-1}. ^{1}H NMR (400 MHz, $CDCl_3$) δ = 11.5 (s, 1H, OH), 8.5 (s, 1H, N_1H), 7.9 (s, 1H, N_3H), 7.4–7.1 (m, 10H, aromatic), 6.9 (d, 1H, J = 16.4, CH=CH), 6.4 (d, 1H, J = 16.5, CH=CH), 5.4 (s, 1H, methine). ^{13}C NMR (200 MHz $CDCl_3$) 50.03, 106.4, 126.1, 126.4, 126.9, 127.1, 127.3, 127.4, 127.6, 127.7, 128.0. LC–MS, m/z 320 M$^+$ (Fig. 1).

2.3. Synthesis of metal complexes

The ligand ADP (2 mM, 320 mg) was dissolved in ethanol (20 mL) and to this metal acetates (1 mM) Mn^{2+}, Cu^{2+}, Ni^{2+}, Zn^{2+} dissolved in ethanol were added slowly, with constant stirring, over a period of 10 min. The reaction mixture was refluxed for 4–8 h. The solid complex obtained was collected on a fine frit filter and dried over fused calcium chloride in a vacuum desiccator. The complexes obtained were MPMC, CPMC, NPMC and ZPMC respectively Mn^{2+}, Cu^{2+}, Ni^{2+}, Zn^{2+} respectively. All complexes with $[Mn(ADP)_2(OAC)_2]^{2-}$, $[Cu(ADP)_2(OAc)_2]^{2-}$, $[Ni(ADP)_2(OAc)_2]^{2-}$ and $[Zn(ADP)_2(OAc)_2]^{2-}$ were obtained by refluxing a mixture of ligand and appropriate metal salts in 2:1 molar ratio in ethanol. The complexes obtained were soluble in acetic acid, DMSO, DMF and sparingly soluble in other common solvents. The physical data of the ligand and complexes are presented in Table 1.

2.4. Characterizations

Microanalysis of pyrimidine based ligand and its metal complexes were performed on a Perkin Elmer Model 240C elemental analyser. IR spectra were obtained on a Perkin Elmer 1800 spectrophotometer using KBr discs. ^{1}H NMR spectra were recorded from $CDCl_3$/DMSO-d_6 solution on a Brucker Avance II 400 (400 MHz) NMR Spectrometer. Chemical shifts are reported as in δ values (ppm) downfield relative to TMS (0.00 ppm) as an internal standard. Magnetic susceptibilities of complexes were measured were by the Gouy's method using $Hg[Co(SCN)_4]$ as calibrant at room temperature. The effective magnetic moments were calculated using the relation:

$$\mu_{eff} = 2.828(\chi mT)^{1/2}\ \text{BM}$$

where χm is the molar susceptibility corrected using Pascal's constants for diamagnetism of all atoms in the compounds.

The TG-DTA measurements were carried out on a Perkin Elmer Thermogravimetric analyser in dry nitrogen atmosphere and at heating rate of 10 °C/min using Pyris program. Mass spectra were measured with a GC–MS (70 eV). The X-ray diffraction patterns have been recorded in 2θ range from 13 to 60° on Philips (Holland) automated X-ray powder diffractometer. The operating target voltage was 35 kV and tube current was 20 mA. The scanning speed was 0.5 2θ/min. Radiation used was Cu-K of wavelength 1.54056 Å provided with a monochromator for filtering β radiations to reduce noise due to white radiations and to increase the resolution. The values of interplaner spacing (d) corresponding to Bragg reflections (2θ) were obtained. Indexing and calculations of unit cell parameters were performed with the help of Powder-X-Software [16,17].

2.5. Screening of antibacterial and antifungal activities

The *in vitro* evaluation of antimicrobial activity was performed according to the diffusion technique [21]. The bacteria including *Staphylococcus aureus* and *Escherichia coli* were grown in nutrient broth at 37 °C for 24 h. *Candidaalbicans* and *Fusarium solani* were grown in malt broth at 28 °C for 48 h. The ligand and its complexes were tested using the diffusion technique on solid media. Sterile (5 mm) diameter sensitivity discs were impregnated with different concentrations of the compounds in DMF (50 μg or 100 μg mL^{-1}). Discs of each tested compound were laid onto nutrient agar for bacteria or potato dextrose agar for fungi. Plates were surface spread with 0.2 mL of logarithmic phase bacteria or fungi cultures. A 0.5 mL spore

Table 1
Physical and analytical data of ligand and metal complexes.

Compound	Molecular composition	Colour	m.p.	Yield (%)	Found (calculated) %		
					C	H	N
Ligand	$C_{19}H_{16}N_2O_3$ MW = 320	Light yellow	220	70	71.22 (71.24)	5.05 (5.03)	8.72 (8.74)
MPMC	$C_{43}H_{38}MnN_4O_{10}$ MW = 825.72	Brown	268	89	62.56 (62.55)	4.67 (4.64)	6.77 (6.79)
CPMC	$C_{42}H_{36}CuN_4O_{10}$ MW = 819.32	Dark brown	287	86	61.49 (61.50)	4.45 (4.42)	6.82 (6.83)
NPMC	$C_{42}H_{36}NiN_4O_{10}$ MW = 815.45	Bluish yellow	265	84	71.25 (71.24)	4.41 (4.45)	6.86 (6.87)
ZPMC	$C_{42}H_{36}ZnN_4O_{10}$ MW = 820.17	Yellow	291	72	61.35 (61.36)	4.43 (4.41)	6.80 (6.81)

Table 2
Characteristics IR bands (cm^{-1}) for ligand and complexes.

Compound	ν(—OH)	ν(C=O)	ν(N—H)	ν(CH_3COO)	ν(M—O)
Ligand	3115	1686	3410, 3231	–	–
CPMC	–	1676	3410,3249	1535,1385	559
NPMC	–	1686	3410,3229	1560,1344	503
ZPMC	–	1686	3405,3228	1568,1344	498
MPMC	–	1688	3402,3232	1508,1390	403

suspension (108 spores mL^{-1}) for bacteria or for filamentous fungi was also spread onto potato dextrose agar plates. The plates were then incubated for 24 h at 37 °C for bacteria and 28 °C for 48 h for fungi. Additionally antibiotic discs for Cephalosporin and/or Streptomycin were tested as positive control. The results were repeated two times and recorded by measuring the zones of growth inhibition surrounding the discs. The mean values of the results are presented in the Table 5.

3. Result and discussion

3.1. IR spectra

The derivatives of carboxylic acids are characterized by several intense absorptions in infrared Spectrum. The most prominent ones are in carbonyl stretching region (1700–1725 cm^{-1}). Their exact position depends on the type of acid derivative. In addition to carbonyl stretching absorption, the acids themselves exhibit a strong, broad —OH stretching at a range from 3500 to 2500 cm^{-1}. Bands at 3231 and 1686 cm^{-1} are characteristic of —OH and C=O group at free ligand. The disappearance of 1686 cm^{-1} band of Cu(II) complex suggests coordination of carboxylic oxygen after deprotonation [20]. The spectrum of free ligand (ADP) attributed to —NH stretching at 3410 and 3115 cm^{-1}. A comparison of IR spectra of complexes with those of free ligands do not display any appreciable shifts in —NH stretching frequencies indicating that —NH groups do not participate in coordination with metal ions. The characteristic bands at 1535 and 1385 cm^{-1} belong to asymmetric (ν_{asym}(COO—)) and symmetric (ν_{sym}(COO—)) vibrations of the acetate groups [22]. The energy separation between (ν_{asym}(COO—)) and (ν_{sym}(COO—)) is found to be >144 cm^{-1} (150–185 cm^{-1}), and this indicates the monodentate nature of the acetate ion [23], since in the event of bidentate coordination, the energy separation is reported to be <144 cm^{-1}. Further, the IR spectra of the complexes exhibit a new band in the far-IR region at 550–560 cm^{-1}. This absorption is assigned to ν(M—O) [24]. The other significant vibrations of Zn(II) and Ni(II) complexes are depicted in Table 2. $[Mn(ADP)_2(OAc)_2]^{2-}$ exhibited an octahedral geometry. The octahedral coordination of manganese ions was confirmed through the evidences provided by IR frequencies of acetate ions. The energy separation of the asymmetric (ν_{asym}(COO—)) and symmetric vibrations (ν_{sym}(COO—)) is found as <144 (1508–1390) cm^{-1} thus indicating that both the —O atoms of acetate ions are involved in coordination as bidentate ligands (Scheme 1) [25].

3.2. NMR spectra

In the ^1H NMR of ADP a singlet at δ 11.5 confirmed the presence of —COOH moiety. N_1 and N_3 protons appeared at δ 8.5 and δ 7.6 as singlets. The multiplets at δ 7.4 to δ 7.1 for 10 aromatic protons indicate the presence of two phenyl rings. Two doublets at δ 6.9 (J = 16.4) and at δ 6.4 (J = 16.5) respectively account for a styryl group. Considering the model of Zn(II) complex, the disappearance of O—H peak at δ 11.5 signifies oxygen–metal bonding. N_1 and N_3 protons appeared at δ 8.5 and δ 7.6 as singlets. Other peaks appear at δ 3.2(s, 6H, acetate H) indicating two acetate ions to be attached to the metal ions. The ligand coordination to metal *via* oxygen atom is evidently strong because of easy deprotonation of the —COOH group. Two singlets at δ 5.1 and δ 4.9 are due to *Si* and *Re* configurations of pyrimidine nuclei.

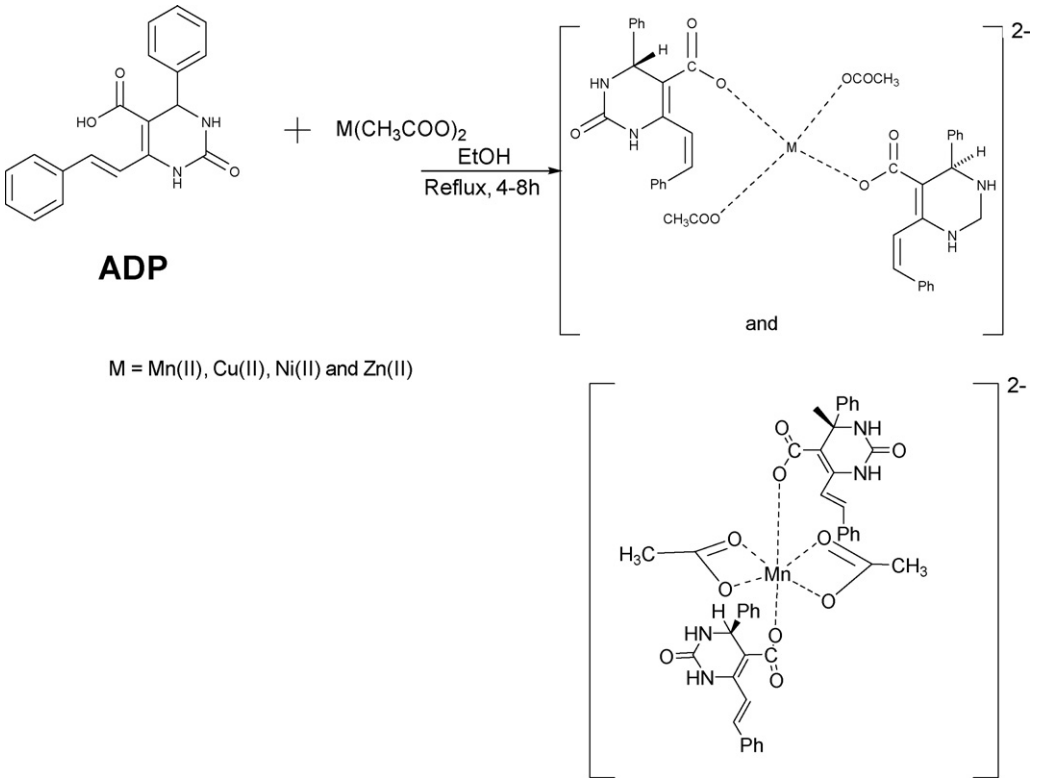

Scheme 1. Synthesis of metal complexes and their suggested structures.

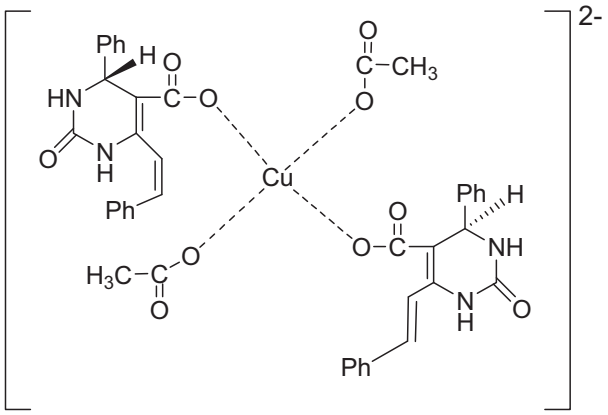

Fig. 2. Suggested geometry of $[Cu(ADP)_2(OAc)_2]^{2-}$.

The ^1H NMR spectral data of ligand was supplemented by ^{13}C NMR spectral data. The chemical shifts for carbon of aromatic rings were recorded between δ 126 and δ 128;the signal for carbon of —COOH group was observed at δ 171.23. Other signals at δ 124 and δ 131 were attributed to styryl carbon atoms. The ^{13}C NMR of all the complexes displayed characteristic signals ranging from δ 22.7–23.1 and δ 176.41–177.28 and thus providing additional evidence for the proposed coordination with —O of acetate ions (Fig. 2).

3.3. Electronic spectra

The electronic spectra of ligand and complexes were recorded in DMF at room temperature. The diamagnetic Zn(II) and Ni(II) complexes had bands in 280–250 nm range due to $n \rightarrow \pi^*$ and $\pi \rightarrow \pi^*$ transitions of benzene, pyrimidine and carbonyl group respectively. In the spectra of complexes, less intense and broad bands in the 445–250 nm range result from overlap of low energy $\pi \rightarrow \pi^*$ transitions and LMCT (ligand to metal charge transfer bands from electronic lone pairs of carboxylate oxygen to the M^{2+} ions.)

The electronic spectra of the Cu(II) complexes (Table 3) are compared with those of the ligands. Two bands appeared at 356 cm^{-1} and 270 cm^{-1}, which can be assigned to $\pi \rightarrow \pi^*$ and $n \rightarrow \pi^*$ transitions, respectively, in the complex. Apart from this a broad band centred at 560 cm^{-1} can be assigned to $d \rightarrow d$ transitions of the metal ions ($^2B_{1g} \rightarrow {}^2A_{1g}$; $^2B_{2g}$) and which strongly favour square-planar geometry around the central metal ion [21]. In addition, the μ_{eff} values for this compound calculated as 1.85 BM, indicative of one unpaired electron per Cu(II) ion and suggesting that the square-planar geometry [26].

Electronic absorption spectra of Ni(II) are characterized by a broad band in the range of 270–300 nm. This behaviour can be assigned to $^1A_{1g} \rightarrow {}^1B_{1g}$ and $^1A_{1g} \rightarrow {}^1E_{1g}$ transitions confirmed square planar geometry of these complexes. The magnetic moment for Ni(II) in complex is zero which is in good agreement with electronic data.

3.4. Molar conductance

The complexes were dissolved in DMF and the molar conductivities of 10^{-3} M of their solutions at room temperature were measured. Table 3 shows the molar conductance values of the complexes. It is concluded from the results that complexes are found to have molar conductance values in the range of 2–14 ohm^{-1} mol^{-1} cm^2 indicating the non-electrolytic nature of these complexes [27].

3.5. Mass spectra

The mass spectra of ligand and the complexes showed peaks attributed to the molecular ions m/z at 320 $[L]^+$, 825 M^+, 815 M^+, 819 M^+ and 820 M^+ for ligand, manganese, copper, nickel and zinc complexes, respectively.

3.6. X-ray powder diffraction analysis

All complexes were found to be crystalline and their X-ray powder diffractograms were collected. The lattice parameters and Miller indices were computed. The indexing and calculation of unit cell parameters are performed with the help of Powder-X Software. The calculated and observed 2θ value, the relative intensity, interplanar distance along with Miller's indices for corresponding angles are tabulated for the complexes. On the basis of X-ray powder patterns and unit cell refinements, it is found that all the complexes adopt triclinic crystal system with p-type of lattice space group. The lattice constants calculated, complex (MPMC) and (CPMC) are depicted in Table 4.

3.7. Themogravimetric analysis

Thermal behavioural analysis of complexes CPMC, NPMC, ZPMC and MPMC were conducted in the temperature range of 23–800 °C with the heating rate of 10 °C/min. The calculated decomposition

Table 3
Electronic spectral data, magnetic moment and geometry for ligand and metal complexes.

Compound	Absorption (nm)	Band assignments	Transitions	Magnetic moment (μ_{eff})	Geometry	Molar Conductance (ohm^{-1} mol^{-1} cm^2)
Ligand	279 256	$n \rightarrow \pi^*$ $\pi \rightarrow \pi^*$				
CPMC	560 356 270	$d \rightarrow d$ Intraligand Intraligand	$^2B_{1g}$–$^6A_{1g}$	1.85	Square planar	2
NPMC	257 243	Intraligand Intraligand		Diamagnetic	Square planar	7.5
ZPMC	283 247	Intraligand Intraligand		Diamagnetic	Square planar	12.3
MPMC	550 401 379	d→d Intraligand Intraligand		5.83	Octahedral	14

Table 4
Powder XRD data of metal complexes.

Data	CPMC	MPMC
Chemical formula	$C_{42}H_{36}CuN_4O_{10}$	$C_{43}H_{38}MnN_4O_{10}$
Molecular weight (g/mol)	819.32	825.72
Crystal system	Triclinic	Triclinic
Space group	P−1	P−1
Unit cell dimensions		
a	4.9168	4.9160
b	4.9865	4.9153
c	5.4089	5.4084
α	78	82
β	90	85
γ	104	115
Volume	132.61	130.68
(Calc.) density (g/cm^{-3})	6.1	6.3
Temperature	299 K	299 K

patterns of the complexes are in agreement with the theoretical data. All complexes decompose in three major phases.

The first phase corresponds to the loss of 2 moles of acetate ions between 100 and 300 °C with mass losses of (obs. = 14.26%, calc. = 14.31%). The second phase is from 305 to 410 °C and is attributed to the loss of the organic moiety of styryl and phenyl ring with mass losses of C_8H_7 (obs. = 24.91%, calc. = 25.1%). The final phase shows the loss of the organic moiety of pyrimidine and phenyl ring of 408 at 450–800 °C with mass losses of (obs. = 49.53%, calc. = 49.33%) leaving metal oxides as residues.

3.8. In vitro biological evaluation

The ligand and its metal complexes were evaluated for antimicrobial activity against one strain Gram positive bacteria (*S. aureus*) (a), Gram negative bacteria(*E. coli*) (b), fungus (*Candida albicans*) (c) and fungus *F. solani* (d) and the results are summarized in Table 5. The ligand was found to be biologically active and their metal complexes enhanced antimicrobial activity against one or more strain. Remarkably, the complexes showed appreciable inhibition against *S. aureus* (a), *C. albicans* (c) and *F. solani* (d) ranging from 43 to 86%. It is known that chelation tends to make the ligand a more powerful and potent bactericidal agent. A possible explanation for the observed increased activity upon chelation is that the positive charge of the metal in chelated complex is partially shared with the ligand's donor atoms so that there is an electron delocalization over the whole chelate ring. This, in turn, will increase the lipophilic character of the metal chelate and favours its permeation through the lipoid layers of the bacterial membranes. Typically, chelated complexes deactivate various cellular enzymes, which play a vital role in various metabolic pathways of these microorganisms. Other factors such as solubility, conductivity and dipole moment which affected by the presence of metal ions, may also be possible reasons for increasing the biological activity of the metal complexes as compared to the corresponding ligand.

Table 5
In vitro antimicrobial activity of ligand and its metal complexes.

Compound	a	b	c	d
Ligand (ADP)	+++	++	+++	++
NPMC	++	+++	+	++
CPMC	+++	+++	++	+
ZPMC	++	+++	++	++
MPMC	+++	+++	++	+
Cephalosporin[a]	++++	+++	+++	++++
Streptomycin[b]	++++	+++	+++	++

a, *S. aureus*; b, *E. coli*; c, *Candida albicans*; d, *F. solani*.
[a] Standard antifungal agent.
[b] Antibacterial agents.
Inhibition zone diameter in nm (% inhibition): (+) 8–10 (36–45%); (++) 10–16 (45–73%); (+++) 16–19 (73–86); (++++). Percent inhibition values are relative to inhibition zone (22 mm) (100%).

4. Conclusion

MPMC, CPMC, NPMC and ZPMC complexes were synthesized and characterized. Analytical data, electronic spectra, magnetic susceptibility, IR and ^{1}H NMR have been revealed octahedral geometry of MPMC and square planar geometry of CPMC, NPMC and ZPMC, respectively. The low conductance values showed non-electrolytic behaviour of the complexes. Single crystals of the compounds could not be isolated; however, powder XRD data, spectroscopic and magnetic data enabled us to elucidate possible structures. The complexes were evaluated *in vitro* for the antibacterial and the antifungal activities. All metal complexes had effective and selective antibacterial activity against bacterial strains. The results speculate regions for higher activity of complexes: (1) the metal complexes could be inactivated to several structural enzymes, catalysing biosynthetic reactions inessential metabolic pathways of the microorganisms; and (2) they act as a whole, are able to cross the cell membranes and interfere with the vital cell mechanisms including DNA replication, transcription, and protein synthesis.

Acknowledgements

RPD gratefully acknowledges UGC, New Delhi for financial assistance under faculty improvement program of XI plan. The authors wish to express their gratitude to the Department of Pharmacy, Nagpur for IR spectroscopic analysis; the Sophisticated Analytical Instrumentation Facility (SAIF), Chandigarh for ^{1}H NMR spectroscopic analysis and mass analysis; and the University of Pune, Pune for ^{13}C NMR spectroscopic data. We also wish to acknowledge Metallurgical and Materials Engg. Department, VNIT, Nagpur for TGA–DTA analysis and Powder XRD; and Department of Chemistry, R.T.M. University, Nagpur for magnetic moment. We do acknowledge Department of Physics, Institute of Science, Nagpur for UV spectral data.

References

[1] A.D. Tiwari, A.K. Mishra, S.B. Mishra, B.B. Mamba, B. Maji, S. Bhattacharya, Spectrochim. Acta A: Mol. Biomol. Spectrosc. 79 (2011) 1050.
[2] S.M. Mamba, A.K. Mishra, B.B. Mamba, P.B. Njobeh, M.F. Dutton, E. Fosso-Kankeu, Spectrochim. Acta A: Mol. Biomol. Spectrosc. 77 (2010) 579.
[3] A.K. Mishra, N.K. Kaushik, Spectrochim. Acta A: Mol. Biomol. Spectrosc. 69 (2008) 842.
[4] A.K. Mishra, N. Manav, N.K. Kaushik, Spectrochim. Acta A: Mol. Biomol. Spectrosc. 61 (2005) 3097.
[5] A.K. Mishra, S.B. Mishra, N. Manav, R. Kumar, Sharad, R. Chandra, D. Saluja, N.K. Kaushik, Spectrochim. Acta A: Mol. Biomol. Spectrosc. 66 (2007) 1042.
[6] N. Manav, A.K. Mishra, N.K. Kaushik, Spectrochim. Acta A: Mol. Biomol. Spectrosc. 65 (2006) 32.
[7] F. Hueso, N.A. Illan, M.N. Moreno, J.M. Martinez, M.J. Ramirez, J. Inorg. Biochem. 94 (2003) 326.
[8] S.P. Fricker, Dalton Trans. (2007) 49030.
[9] T.W. Hambley, Dalton Trans. (2007) 4929.
[10] P.G. Baraldi, M.G. Pavani, N. Nunes, P. Brigidi, B. Vitali, R. Gambari, R. Romagnoli, Arch. Pharm. 10 (2002) 449.
[11] S.M. Sondhi, M. Johar, S. Rajvanshi, S.G. Dastidar, R. Shukla, R. Raghubir, J.W. Lown, Aust. J. Chem. 54 (2001) 69.
[12] M.N. Nasr, M.M. Gineinah, Arch. Pharm. 335 (2002) 289.
[13] N. Kumar, G. Singh, A.K. Yadav, Heteroat. Chem. 12 (2001) 52.
[14] G. Mangalagiu, M. Ungureanu, G. Grosu, L. Mangalagiu, M. Petrovanu, Ann. Pharm. Fr. 59 (2001) 139.
[15] M. Sönmeza, M. Çelebib, A. Leventb, İ. Berberc, Z. Şentürkb, J. Coord. Chem. 63 (2010) 1986.
[16] Azaroff, Buerger, The Powder Method, McGraw Hill, London, 1958.

[17] W.H. Bragg, W.L. Bragg, The Powder Method, Bell, London, 1953.
[18] P. Biginelli, Gazz. Chim. Ital. 23 (1893) 360.
[19] C.H. Collins, P.M. Lyne, Microhiul Melfwds, University Park Press, Baltimore, 1970, p. 422.
[20] M. Sönmez, Turk. J. Chem. 25 (2001) 181.
[21] M.B. Ferrari, S. Capacchi, G. Pelosi, P. Tarasconi, R. Alberitini, S. Pineli, P. Lunghi, Inorg. Chim. Acta 134 (1999) 286.
[22] D. Kumar, P.K. Gupta, A. Syamal, J. Chem. Sci. 117 (2005) 247.
[23] V. Ravinder, S.J. Swamy, S. SriHari, P. Lingaiah, Polyhedron 4 (1985) 1511.
[24] K. Nakamoto, Infrared and Raman Spectra of Inorganic and Coordination Compounds, Wiley, New York, 1978.
[25] S.J. Swamy, E.R. Reddy, D.N. Raju, S. Jyothi, Molecules 11 (2006) 1000.
[26] E. Yousif, H. Adil, Y. Farina, J. Appl. Sci. Res. 6 (2010) 879.
[27] U.M. Rabie, A.S.A. Assram, M.H.M. Abou-EI-Wafa, J. Mol. Struct. 872 (2008) 113.